Calculated optical properties of Si, Ge, and GaAs under hydrostatic pressure

M. Alouani and J. M. Wills
Department of Physics, Ohio State University, Columbus Ohio 43210-1368
Theoretical Division, Los Alamos National Laboratory, Los Alamos, New Mexico 87545
(Received 7 March 1996)

The macroscopic dielectric function in the random-phase approximation without local-field effect has been implemented using the local-density approximation with an all-electron, full-potential linear muffin-tin orbital basis set. This method is used to investigate the optical properties of the semiconductors Si, Ge, and GaAs under hydrostatic pressure. The pressure dependence of the effective dielectric function is compared with the experimental data of Goñi, Syassen, and Cardona [Phys. Rev. B **41**, 10 104 (1990)], and excellent agreement is found when the so-called ''scissors-operator'' shift is used to account for the correct band gap at Γ. The effect of the $3d$ semicore states in the interband transitions hardly changes the static dielectric function ϵ_∞; however, their contribution to the intensity of absorption for higher photon energies is substantial. The spin-orbit coupling has a significant effect on ϵ_∞ of Ge and GaAs, but not of Si. The E_1 peak in the dynamical dielectric function is strongly underestimated for Si, but only slightly for Ge and GaAs, suggesting that excitonic effects might be important only for Si.[S0163-1829(96)04828-X]

I. INTRODUCTION

The experimental determination of the optical properties of bulk semiconductors can now be obtained with high precision,[1–3] yet our theoretical understanding is far from complete. The static dielectric constant, which can be obtained from a functional derivative of the electron density with respect to the total Kohn-Sham potential evaluated at the ground state, hence a ground-state property, is overestimated by the local-density approximation (LDA) calculation.[4–6] The inclusion of the gradient correction to the pseudopotential LDA reduces slightly the discrepancy in the case of silicon.[7] The underestimation of the E_1 peak and the overestimation of the E_2 peak of the imaginary part of the dielectric function, $\epsilon_2(\omega)$, by one-electron band theory have generated theoretical work for almost two decades to account for these discrepancies. It was clear from the beginning that including excitonic effects, which have been detected experimentally,[8] could remove some of the disagreement with experiment.[9–12] However, the model calculations used to correct $\epsilon_2(\omega)$ have produced only a qualitative understanding of the problem. In particular, the latest model by Hanke, Mattausch, and Strinati based on the time-dependent screened Hartree-Fock approximation and including both the local-field and the excitonic effects described correctly the E_1 peak but underestimated significantly the E_2 peak of Si. The reason for the underestimation of E_2 was attributed to a bad representation of the band structure of Si by their Slater-Koster parametrization.[11] del Castello-Mussot and Sham[12] based their latest calculation on a $\mathbf{k}\cdot\mathbf{p}$ model around the L point (where E_1 originates) and a multiple plane-wave model around the X points (where E_2 originates) and solved the Bethe-Salpeter equation containing the excitonic effect. Their model is an improvement over the noninteracting approximation: the E_1 peak becomes stronger and the E_2 peak weaker. This model is very promising, but, being based on a $\mathbf{k}\cdot\mathbf{p}$ approximation to the band structure, it provided only a qualitative correction to the intensities of the E_1 and E_2 structures. Calculations ignoring excitonic effects, but including the local-field effect, underestimated both E_1 and E_2 peaks.[13] However, the most recent calculation of Engel and Farid,[40] which uses a continued fraction expansion of the polarizability and a representation of the inverse dielectric function in terms of plasmonlike excitations, overestimated the E_2 peak, and produced a sharp peak at 2.8 eV not observed by experiment.

One way to make theoretical progress in this field is to determine the correct contribution of the one-electron theory to the optical properties of semiconductors. This allows us to define precisely the size of the many-body corrections to the one-electron theory. However, a common belief these days is that the eigenvalues and vectors of the Kohn-Sham (KS) equations[14] have no direct physical meaning and hence should not be used to calculate optical spectra of materials. Only ground-state properties derived from the total energy as a function of the electron density have, in principle, a direct physical meaning.

While LDA was indeed intended to calculate ground-state properties it could also be viewed as a simplified quasiparticle (QP) theory where the self-energy is local and static [$\Sigma(\mathbf{r},\mathbf{r}',t)\approx V_{\rm xc}(\mathbf{r})\delta(\mathbf{r}-\mathbf{r}')\delta(t)$, here $V_{\rm xc}(\mathbf{r})$ is the local exchange and correlation potential as parametrized, for example, by Von Barth and Hedin[15]]. The KS eigenvalues are then QP energies and could be compared to experimental data. This argument is supported by calculations using the GW approximation of Hedin.[16] These calculations showed that the valence QP energies of semiconductors are in good agreement with LDA and the conduction QP energies differ by approximately a rigid energy shift.[17,18] In the literature this shift is often called a ''scissors-operator'' shift (SOS).[6]

First-principles local-density approximation calculations started more than two decades ago, but the major problem of LDA, beside the well understood energy-band-gap problem,[19] is the numerical difficulty in determining self-consistent electronic-structure and optical matrix elements using a complete basis set. The early *ab initio* calculation of

the optical properties of semiconductors by Wang and Klein, using a self-consistent linear combination of Gaussian orbitals, produced static dielectric functions in good agreement with experiment.[20] But this agreement is fortuitous because the band gaps produced by this method are much larger than the LDA band gaps. The recent calculations of 18 semiconductors by Huang and Ching using an orthogonalized linear combination of atomic orbitals method produced LDA static dielectric functions that are, in general, smaller than experiment despite the fact that their band gaps are much larger than the all-electron or pseudopotential LDA band gaps.[21] Those underestimated static dielectric constants are most likely due to the incompleteness of the basis set used in their calculations.

Most of the theoretical studies of the optical properties of semiconductors in the literature use several approximations within the LDA, ranging from the use of spherical potentials[5] to the use of pseudopotentials[6] instead of all electron LDA potentials. In this paper we report precise calculations of the optical properties of bulk semiconductors Si, Ge, and GaAs under hydrostatic pressure using an all-electron LDA linear muffin-tin orbital (LMTO) basis set,[22] in which no shape approximation is made for either the potential or the charge density.[23] The semicore $3d$ of Ga and Ge are included in a fully hybridizing valence basis set and the rest of the core states are allowed to relax self-consistently. The effect of spin-orbit coupling is also investigated. A systematic check of the f-sum rule is performed for all the calculations. We hope that this accurate LDA calculation will provide an excellent starting point for the determination of the local-field and the excitonic effects in the optical spectra of semiconductors.[9–13]

We have found that the static dielectric function ϵ_∞, which is a ground-state property, is overestimated by LDA over all pressure range and that excellent agreement with the experimental results of Goñi, Syassen, and Cardona[1] for ϵ_∞ of GaAs and Ge under hydrostatic pressure is achieved only when the so-called scissors-operator shift is used to account for the correct band gap at Γ. The inclusion of the $3d$ semicore states of Ge and GaAs in the interband transition has almost no significant effects in ϵ_∞; however, the $3d$ interband transitions contribute significantly to the magnitude of $\epsilon_2(\omega)$ above 25 eV for Ge and above 12 eV for GaAs. The spin-orbit coupling increases the LDA values by about few percent.

The rest of the paper is organized as follows. In Sec. II we describe the method of the calculation of electronic structure and the macroscopic dielectric function based on our all-electron full-potential LMTO basis set. In Sec. III we present the electronic properties of Si, Ge, and GaAs and compare them to existing theoretical results. The calculated dielectric functions and a discussion about including the semicore states and the spin-orbit coupling will be presented in Sec. IV. In the same section we also compare our static dielectric function under hydrostatic pressure with the experimental results of Goñi, Syassen, and Cardona.[1] The conclusion is given in Sec. V.

II. METHOD OF CALCULATION

A. All-electron full-potential wave function

The full-potential linear muffin-tin orbital method in its scalar-relativistic and full-relativistic forms[23] is used here to calculate the electronic structure and the optical properties of Si, Ge, and GaAs under hydrostatic pressure. The Kohn-Sham[14] equations are solved for a general potential without any shape approximation.[23] In this subsection we describe the Bloch wave function inside the so-called muffin-tin spheres and the interstitial region. A correct determination of the crystal wave function is necessary for the accurate determination of the optical matrix elements.

As for the cellular methods, the space is divided into nonoverlapping muffin-tin spheres surrounding atomic sites where the Schrödinger or the Dirac equation for each principle quantum number ν and momentum channel ℓ is solved for a fixed energy $E_{\nu\ell}$. In these muffin-tin spheres the trial wave function is linearized in terms of the solution of Schrödinger equation $\phi_{\tau\ell}$ and its energy derivative $\dot{\phi}_{\tau\ell}$ for the energy $E_{\nu\ell}$, and for an atom of type τ and momentum channel ℓ.[22,24]

It can be shown that the Bloch wave function of site τ calculated at site τ' in the unit cell of the crystal at $\mathbf{R}=\mathbf{0}$ is given by:[23]

$$\chi^{\mathbf{k}}_{\tau\ell m}(\mathbf{r})|_{\tau'} = \sum_{\ell' m'} \phi_{\tau'\ell' m'}(\mathbf{r}-\tau') B^{(1)\tau\tau'}_{\ell' m',\ell m}(\kappa,\mathbf{k}) + \dot{\phi}_{\tau'\ell' m'}(\mathbf{r}-\tau') B^{(2)\tau\tau'}_{\ell' m',\ell m}(\kappa,\mathbf{k}), \quad (1)$$

where $B^{(1)\tau\tau'}_{\ell' m',\ell m}(\kappa,\mathbf{k})$ and $B^{(2)\tau\tau'}_{\ell' m',\ell m}(\kappa,\mathbf{k})$ are renormalized structure constants obtained from the crystal structure constants $B^{\tau\tau'}_{\ell' m',\ell m}(\kappa,\mathbf{k})$ to ensure that the Bloch wave function is continuous and differentiable at the boundary of each muffin-tin sphere.

In the interstitial region, the muffin-tin orbitals are spherical wave solutions H_ℓ to the Helmholtz equation with nonzero kinetic energy; these bases are Hankel functions for negative kinetic energies or Neumann functions for positive kinetic energies κ^2 such that each partial wave inside the muffin-tin sphere is allowed to have different kinetic energy κ^2 in the interstitial region. In this region the Bloch wave function is given by

$$\chi^{\mathbf{k}}_{\tau\ell m}(\mathbf{r}) = \sum_{\mathbf{R}} e^{i\mathbf{k}\cdot\mathbf{R}} H_\ell(\kappa,|\mathbf{r}-\tau-\mathbf{R}|) i^\ell Y_{\ell m}(\widehat{\mathbf{r}-\tau-\mathbf{R}}). \quad (2)$$

The interstitial-region Bloch function is expressed in plane waves over the reciprocal lattice using a Fourier transform

$$\chi^{\mathbf{k}}_{\tau\ell m}(\mathbf{r}) = \sum_{\mathbf{G}} f_{\mathbf{K}}(\mathbf{k}+\mathbf{G}) e^{i(\mathbf{k}+\mathbf{G})\cdot\mathbf{r}}, \quad (3)$$

where $\mathbf{K}=\{\tau,\ell,m,E_\ell,\kappa\}$, with the parameter E_ℓ being the linearization energy of the wave function in the muffin-tin sphere for the ℓ momentum channel, m the azumutal quantum number, and κ the variational parameter whose square is the kinetic energy in the interstitial region. The Fourier coefficients $f_{\mathbf{K}}$ are obtained from a pseudowave function that is equal to the crystal wave function in the interstitial region and represented by a smooth function inside the muffin-tin spheres. The exact shape of these pseudofunctions inside the muffin-tin spheres is not important. The only requirement is that they are continuous and differentiable at the sphere

TABLE I. Basis sets used for the calculation of the excited states of Si, Ge, and GaAs. Each orbital has different kinetic energy κ^2 in its the interstitial region. For example, the 3*s* orbital of Si is used three times and each of the 3*s* wave functions has a different kinetic energy in the interstitial region.

Semiconductor	Basis set
Si	$3\times(3s,3p)$, $2\times(3d)$
	$3\times(4s,4p)$, $2\times(4d,4f)$
Ge	$2\times(3d)$,
	$3\times(4s,4p)$, $2\times(4d)$,
	$2\times(5s,5p)$,
GaAs	$2\times(\mathrm{Ga}3d)$
	$3\times(\mathrm{Ga}4s,4p)$, $2\times(\mathrm{Ga}4d)$
	$3\times(\mathrm{Ga}5s,5p)$,
	$3\times(\mathrm{As}4s,4p)$, $2\times(\mathrm{As}4d)$,
	$3\times(\mathrm{As}5s,5p)$

boundary and have zero slope at the origin of each sphere. The plane-wave expansion is multiplied by a three-dimensional step function so that the wave function is kept only in the interstitial region. The knowledge of the Bloch wave function in the whole unit cell allows us to calculate the Hamiltonian and overlap matrix elements in order to solve the effective one-electron Schrödinger equation.

Three different kinetic energies were used for each subset of *s* and *p* derived bases in the basis set; two kinetic energies were used for bases derived from orbital parameters $\ell > 1$. The basis sets used in calculating total energies and structural properties were, for Si, 3(3*s*3*p*) and 2(3*d*); for Ge, 2(3*d*), 3(4*s*4*p*), and 2(4*d*); and for GaAs, 2(Ga 3*d*), 3(Ga 4*s*4*p*), 2(Ga 4*d*), 3(As 4*s*4*p*), and 2(As 4*d*); the premultiplicities in this notation refer to the number kinetic energies used in this basis subset. The basis functions for each material comprised a single, fully hybridizing basis set. Note the presence of both 3*d* and 4*d* derived bases on Ga and Ge. A useful feature of the method used in these calculations is the ability to incorporate basis functions derived from the same orbital atomic quantum numbers but different principal atomic quantum numbers in a single fully hybridizing basis set. This feature entails the use of multiple sets of radial functions to represent bases with different principle atomic quantum numbers. This capability was particularly useful in calculating the high-lying energy bands that were used to obtain the dielectric functions to high energy; the basis sets employed for this purpose are given in Table I. Seven to eight kinetic energies were used in the basis sets. Accurate resolution of the bands to high energy was necessary to converge the calculation of the real part of the dielectric function, which was obtained from the imaginary part through the Kramers-Kronig relation. An interesting consequence of the relaxation of the Ga 3*d* states as valence states is a significant decrease in the calculated band gap.[25]

For the core charge density, the Dirac equation is solved self-consistently, e.g., no frozen core approximation is used. The exchange and correlation potential is treated within the Von Barth–Hedin parametrization.[15] To account for the relativistic effects in the dielectric function, the full-self-consistent relativistic band structure is produced by including the spin-orbit coupling to the Hamiltonian. In Table I we show the orbitals used to describe the electronic states of Si, Ge, and GaAs. This large number of orbitals is necessary to calculate accurately the eigenvalues and eigenvectors up to 5 Ry above the highest valence states. These electronic states will be needed to determine the dynamical dielectric function and the converged static dielectric function through the use of Kramers-Kronig relations.

TABLE II. Eigenvalues of Si at high symmetries points (Γ, X, and L) as compared to the results produced by means of a linear combination of Gaussian orbitals (Ref. 28) and by the pseudopotential (PP) method (Ref. 27). The zero of energy is chosen at the $\Gamma_{25v'}$ point.

High-symmetry point	Gaussian orbitals	PP	Present calculation
Γ_{1v}	−11.91	−11.91	−11.96
$\Gamma_{25v'}$	0.0	0.0	0
Γ_{15c}	2.57	2.55	2.56
$\Gamma_{2c'}$	3.24	3.28	3.20
X_{1v}	−7.77	−7.76	−7.82
X_{4v}	−2.78	−2.86	−2.83
X_{1c}	0.65	0.66	0.62
X_{4c}	10.03		10.03
$L_{2v'}$	−9.58	−9.56	−9.63
L_{1v}	−6.94	−6.96	−6.99
$L_{3v'}$	−1.17	−1.20	−1.19
L_{1c}	1.47	1.50	1.44
L_{3c}	3.32	3.33	3.31
$L_{2c'}$	7.77		7.66
Indirect band gap	0.52		0.50

The completeness of basis set, with different variational κ values for each partial wave in the interstitial region together with the Fourier representation, allows the method to treat open structures such as the zinc-blende structure studied here without having to resort to the so-called empty spheres.[26] The high-energy states are also determined more accurately due to the use of many κ values. As a test we show in Table II the eigenvalues of Si at high symmetry points of the Brillouin zone compared with some recent results from first-principle calculations based on *ab initio* pseudopotential and Gaussian orbital methods.[27,28] The agreement of our calculation with the previous calculations is excellent.

B. Dielectric function

Here we give a concise review of the determination of the dielectric function of a semiconductor crystal due to the application of an electric field. We also determine the approximations used to obtain numerical results for Si, Ge, and GaAs under hydrostatic pressure with or without scissors-operator shift.

A perturbative electromagnetic field of frequency ω and a wave vector $\mathbf{q}+\mathbf{G}$ on a crystal produces a response of frequency ω and a wave vector $\mathbf{q}+\mathbf{G}'$ ($\mathbf{G}$ and $\mathbf{G}'$ being recip-

rocal lattice vectors). The microscopic field of wave vector $\mathbf{q}+\mathbf{G}'$ is produced by the umklapp processes as a result of the applied field $E_0(\mathbf{q}+\mathbf{G},\omega)$

$$E_0(\mathbf{q}+\mathbf{G},\omega)=\sum_{\mathbf{G}'}\epsilon_{\mathbf{G},\mathbf{G}'}(\mathbf{q},\omega)E(\mathbf{q}+\mathbf{G}',\omega), \tag{4}$$

where $E(\mathbf{q}+\mathbf{G},\omega)$ is the total field that produces the nondiagonal elements in the microscopic dielectric function $\epsilon_{\mathbf{G},\mathbf{G}'}(\mathbf{q},\omega)$. In the random-phase approximation the microscopic dielectric function is given by[29]

$$\begin{aligned}\epsilon_{\mathbf{G},\mathbf{G}'}(\mathbf{q},\omega)=\delta_{\mathbf{G},\mathbf{G}'}-\frac{8\pi e^2}{\Omega|\mathbf{q}+\mathbf{G}||\mathbf{q}+\mathbf{G}'|}\\ \times\sum_{\mathbf{k},n,n'}\frac{f_{n',\mathbf{k}+\mathbf{q}}-f_{n,\mathbf{k}}}{E_{n',\mathbf{k}+\mathbf{q}}-E_{n,\mathbf{k}}-\hbar\omega+i\delta}\\ \times\langle n',\mathbf{k}+\mathbf{q}|e^{i(\mathbf{q}+\mathbf{G})\cdot\mathbf{r}}|n,\mathbf{k}\rangle\\ \times\langle n,\mathbf{k}|e^{-i(\mathbf{q}+\mathbf{G}')\cdot\mathbf{r}}|n',\mathbf{k}+\mathbf{q}\rangle.\end{aligned} \tag{5}$$

Here n and n' are the band indices, $f_{n,\mathbf{k}}$ is the zero-temperature Fermi distribution, and Ω is the cell volume. The energies $E_{n,\mathbf{k}}$ and the the crystal wave function $|n,\mathbf{k}\rangle$ are produced for each band index n and for each wave vector $\mathbf{k}$ in the Brillouin zone.

The macroscopic dielectric function in the infinite-wavelength limit is given by the inversion of the microscopic dielectric function

$$\begin{aligned}\epsilon(\omega)&=\lim_{\mathbf{q}\to\mathbf{0}}\frac{1}{[\epsilon^{-1}_{\mathbf{G},\mathbf{G}'}(\mathbf{q},\omega)]_{\mathbf{0},\mathbf{0}}}\\ &=\epsilon_{0,0}(\omega)-\lim_{\mathbf{q}\to\mathbf{0}}\sum_{\mathbf{G},\mathbf{G}'\neq\mathbf{0}}\epsilon_{0,\mathbf{G}}(\mathbf{q},\omega)T^{-1}_{\mathbf{G},\mathbf{G}'}(\mathbf{q},\omega)\\ &\quad\times\epsilon_{\mathbf{G}',\mathbf{0}}(\mathbf{q},\omega),\end{aligned} \tag{6}$$

where $T^{-1}_{\mathbf{G},\mathbf{G}'}$ is the inverse matrix of $T_{\mathbf{G},\mathbf{G}'}$ containing the elements $\epsilon_{\mathbf{G},\mathbf{G}'}$ with $\mathbf{G}$ and $\mathbf{G}'\neq\mathbf{0}$. The first term of this equation is the interband contribution to the macroscopic dielectric function and the second term represents the local-field correction to ϵ. The most recent *ab-initio* pseudopotentials calculation found that the local-field effect reduces the static dielectric function by at most 5%.[6] Previous calculations with the same method have also found a decrease of ϵ_∞ by about the same percentage.[4,17] We are looking at the effect of the local field using our all-electron basis set; it should be of interest to compare all-electron results with these obtained using the pseudopotential method.

For insulators the dipole approximation of the imaginary part of the first term of Eq. (7) is given by[30]

$$\begin{aligned}\epsilon_2(\omega)=\frac{e^2}{3\omega^2\pi}\sum_{n,n'}\int d\mathbf{k}|\langle n,\mathbf{k}|\mathbf{v}|n',\mathbf{k}\rangle|^2 f_{n,\mathbf{k}}\\ \times(1-f_{n',\mathbf{k}})\,\delta(e_{\mathbf{k},n',n}-\hbar\omega).\end{aligned} \tag{7}$$

Here $\mathbf{v}$ is the velocity operator [in the LDA $\mathbf{v}=\mathbf{p}/m$ ($\mathbf{p}$ being the momentum operator)] and $e_{\mathbf{k},n,n'}=E_{n',\mathbf{k}}-E_{n,\mathbf{k}}$. The matrix elements $\langle n\mathbf{k}|\mathbf{p}|n'\mathbf{k}\rangle$ are calculated for each projection $p_j=\hbar/(i)\,\partial_j$, $j=x$ or y, or z, with the wave function $|n\mathbf{k}\rangle$ expressed in terms of the full-potential LMTO crystal wave function described by Eqs. (1) and (3). The $\mathbf{k}$-space integration is performed using the tetrahedron method[31] with 480 irreducible $\mathbf{k}$ points in the whole Brillouin zone. The irreducible $\mathbf{k}$ points are obtained from a shifted $\mathbf{k}$-space grid from the high-symmetry planes and Γ point by a half step in each of the k_x, k_y, and k_z directions. This scheme produces highly accurate integration in the Brillouin zone by avoiding high-symmetry points.

To calculate these matrix elements we first defined a tensor operator of order one out of the momentum operator $\nabla_0=\nabla_z=\partial/\partial z$ and $\nabla_{\pm1}=\mp1/\sqrt{2}\,(\partial/\partial x\pm i\,\partial/\partial y)$. The muffin-tin part of the momentum matrix elements is calculated using the commutator $[\nabla^2,x_\mu]=2\nabla_\mu$ so that

$$\begin{aligned}\int_{S_\tau}d\mathbf{r}\phi_{\tau\ell'}(r)Y_{\ell'm'}(\widehat{\mathbf{r}-\tau})\nabla_\mu\phi_{\tau\ell}(r)Y_{\ell m}(\widehat{\mathbf{r}-\tau})\\ =-\frac{i}{2}G^{1\mu}_{\ell m,\ell' m'}\int_0^{S_\tau}r^2dr\,\phi_{\tau\ell'}\\ \times\left(\frac{2}{r}\frac{d}{dr}r+\frac{\ell(\ell+1)-\ell'(\ell'+1)}{r}\right)\phi_{\tau\ell}(r),\end{aligned} \tag{8}$$

where $G^{1\mu}_{\ell m,\ell' m'}$ are the usual Gaunt coefficients and S_τ is the radius of the muffin-tin sphere of atom τ. In the interstitial region the plane-wave representation of the wave function [see Eq. (3)] makes the calculation straightforward, but special care has to be taken for the removal of the extra contribution in the muffin-tin spheres. However, we find it much easier and faster to transform the interstitial matrix elements as an integral over the surface of the muffin-tin spheres using the commutation relation of the momentum operator and the Hamiltonian in the interstitial region. The calculation of the interstitial momentum matrix elements is then similar to the calculation of the interstitial overlap matrix elements.[23] The $\kappa=0$ case has been already derived by Chen using the Korringa-Kohn-Rostoker Green's-function method.[32] We have tested that both the plane-wave summation and the surface integration provide the same results.

Equation (7) cannot be used directly to determine the optical properties of semiconductors, when the *GW* approximation or the scissors operator is used to determine the electronic structure. The velocity operator should be obtained from the effective momentum operator $\mathbf{p}^{\rm eff}$, which is calculated using the self-energy operator $\Sigma(\mathbf{r},\mathbf{p})$ of the system[33]

$$\mathbf{v}=\mathbf{p}^{\rm eff}/m=\mathbf{p}/m+\partial\Sigma(\mathbf{r},\mathbf{p})/\partial\mathbf{p}. \tag{9}$$

GW calculations show that the quasiparticle wave function is almost equals to the LDA wave function.[17,18] Based on this assumption, Del Sole and Girlanda show that the effective momentum operator $\mathbf{p}^{\rm eff}$ can be written in terms of the momentum operator $\mathbf{p}$ as[33]

$$\langle n',\mathbf{k}|\mathbf{p}^{\rm eff}|n,\mathbf{k}\rangle=\langle n',\mathbf{k}|\mathbf{p}|n,\mathbf{k}\rangle e^{\rm QP}_{\mathbf{k},n',n}/e_{\mathbf{k},n',n}, \tag{10}$$

where $e^{\rm QP}_{\mathbf{k},n',n}=E^{\rm QP}_{n',\mathbf{k}}-E^{\rm QP}_{n,\mathbf{k}}$ is the difference between the quasiparticle energy $E^{\rm QP}_{n',\mathbf{k}}$ of the unoccupied state $|n',\mathbf{k}\rangle$ and the occupied state $|n,\mathbf{k}\rangle$. By substituting Eq. (10) into Eq.

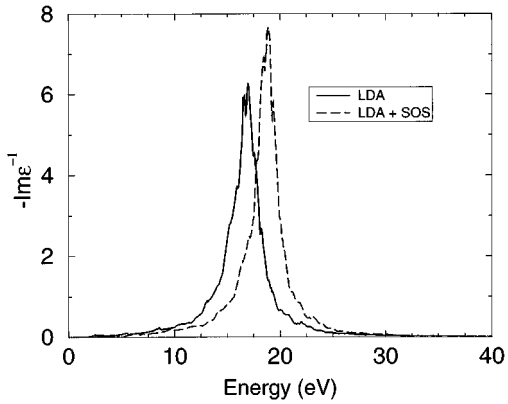

FIG. 1. Calculated energy-loss function of GaAs within the LDA (full curve) and within the scissors approximation (dashed curve). It is clearly seen that the maximum of the LDA curve is much closer to the free valence electron plasma frequency of 15.5 eV.

(7), it can be easily shown[33] that in the case of the scissors operator, where all the empty states are shifted rigidly by a constant energy Δ, the imaginary part of the dielectric function is a simple energy shift of the LDA dielectric function towards the high energies by an amount Δ, i.e., $\epsilon_2^{\mathrm{QP}}(\omega)=\epsilon_2^{\mathrm{LDA}}(\omega-\Delta/\hbar)$. The real part of the dielectric function is then obtained from the shifted ϵ_2 using Kramers-Kronig relations. The expression of $\epsilon_\infty^{\mathrm{QP}}$ is given by

$$\epsilon_\infty^{\mathrm{QP}}=1+\frac{2e^2}{3\omega^2\pi^2}\sum_{n,n'}\int d\mathbf{k} f_{n,\mathbf{k}}(1-f_{n',\mathbf{k}}) \times\frac{|\langle n,\mathbf{k}|\mathbf{p}|n',\mathbf{k}\rangle|^2}{(e_{\mathbf{k},n',n}+\Delta)e_{\mathbf{k},n',n}^2}. \quad (11)$$

$\epsilon_\infty^{\mathrm{QP}}$ is very similar to $\epsilon_\infty^{\mathrm{LDA}}$ except that one of the interband gap $e_{\mathbf{k},n',n}$ is substituted by the QP interband gap $e_{\mathbf{k},n',n}+\Delta$.

To test for the accuracy of the calculation within the LDA the *f*-sum rule,

$$\frac{2}{3mn_v}\sum_{\mathbf{k}}\sum_{n,n'} f_{n,\mathbf{k}}(1-f_{n',\mathbf{k}})\frac{|\langle n,\mathbf{k}|\mathbf{p}|n',\mathbf{k}\rangle|^2}{e_{\mathbf{k},n',n}}=1, \quad (12)$$

where n_v is the number of valence bands, is checked in all the calculations and it is satisfied to within a few percent.

It is easily seen that the dielectric function ϵ_2^{QP} calculated using the scissors-operator shift does not satisfy the sum rule (ω_P is the free-electron plasmon frequency)

$$\int_0^\infty \omega\epsilon_2(\omega)d\omega=\frac{\pi}{2}\omega_P^2 \quad (13)$$

because (i) $\epsilon_2^{\mathrm{LDA}}$ satisfies this rule and (ii) ϵ_2^{QP} is obtained by a simple shift of $\epsilon_2^{\mathrm{LDA}}$ by the scissors-operator Δ towards higher energies. Using the expression of the quasiparticle dielectric function in the scissors-operator shift approximation we show that ϵ_2^{QP} satisfies the integral sum rule

$$\int_0^\infty \omega\epsilon_2^{\mathrm{QP}}(\omega)d\omega=\frac{\pi}{2}(\omega_P')^2, \quad (14)$$

where

$$(\omega_P')^2=\omega_P^2+\frac{2e^2\Delta}{3\pi^2m^2}\sum_{n,n'}$$

TABLE III. Calculated equilibrium volume (V), electronic pressure, and bulk modulus of Si, Ge, and GaAs. The bulk moduli are calculated both at the experimental (V_0) and theoretical (V) unit cell volumes. The experimental results are shown in parentheses.

Semiconductor	V_0 (Å ^{3})	V/V_0	$P(V_0)$ (GPa)	$B(V)$ (GPa)	$B(V_0)$ (GPa)
Si	39.98	0.990	−0.70	95.8	91.2 (98.8)
Ge	45.27	0.988	−0.80	71.0	67.1 (74.4)
GaAs	45.12	0.984	−1.2	74.2	69.3 (74.7)

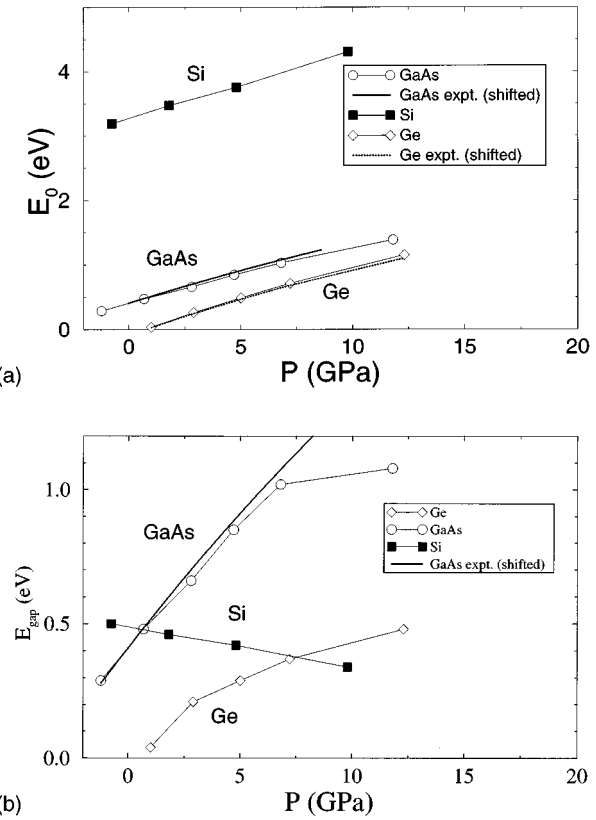

FIG. 2. Calculated (a) direct band gap E_0 and (b) minimum band gap E_{gap} of Si, Ge, and GaAs as a function of hydrostatic pressure compared to the experimental results of Goñi, Syassen, and Cardona (Ref. 1) for Ge (dashed line) and GaAs (thick line). (a) shows that the direct band gaps increase almost linearly with pressure. (b) shows that for GaAs there is a crossover of the band gap from direct to indirect at around 8 GPa and a crossover for Ge at almost 3 GPa. The indirect band gap of Si decreases linearly with pressure.

TABLE IV. First- and second-order coefficients describing the dependence of the direct band gap at Γ (E_0) under hydrostatic pressure [$E_0(P)=E_0+aP+bP^2$] for Si, Ge, and GaAs. The experimental results are from Goñi, Syassen, and Cardona (Ref. 1).

	E_0		a (meV/GPa)		b (meV/GPa^2)	
Semiconductor	Theor.	Expt.	Theor.	Expt.	Theor.	Expt.
Si	3.273		100.8		0.05	
Ge	−0.084	0.795	125.4	121	0.2	0.2
GaAs	0.41	1.43	99.1	108	−0.1	−0.1

$$\times \int d\mathbf{k} |\langle n,\mathbf{k}|\mathbf{p}|n',\mathbf{k}\rangle|^2 / e^2_{\mathbf{k},n',n} f_{n,\mathbf{k}}(1-f_{n',\mathbf{k}}).$$

We recover the usual sum rule when Δ is equal to zero. The nonsimultaneous satisfaction of both the f sum rule and the integral sum rule given by Eq. (13) within the scissors approximation shows the limitation of this approximation. While the scissors-operator approximation describes nicely the low-lying excited states, which is seen in the good determination of the static dielectric function and the low-energy structures, i.e., E_1 and E_2, in the imaginary part of the dielectric function, it seems to fail for the description of the higher excited states. This is not surprising because the higher excited states that are free-electron-like are most probably well described by LDA and need no scissors-operator shift. This is supported by the fact that the energy-loss function $-\mathrm{Im}\epsilon^{-1}$ within the LDA has it maximum roughly at the free-electron plasmon frequency, whereas within the scissors approximation its maximum is shifted to higher energies as given by Eq. (14). Figure 1 show the energy-loss function of GaAs calculated within LDA (full curve) and within the scissors approximation (dashed curve). It is clearly seen that the maximum of the LDA curve has a maximum that is closer to the free valence electron plasma frequency of 15.5 eV. It is of general interest to see whether the calculated dielectric function within the GW approximation satisfies the integral sum rule. For our purpose the scissors-operator shift remains a good approximation for the description of the low-lying excited states of semiconductors and their optical properties.

III. ELECTRONIC STRUCTURE OF Si, Ge, AND GaAs

The electronic structure of Si, Ge, and GaAs are obtained by solving the LDA equations by means of a full-potential LMTO basis set as described above. Table I shows the or-

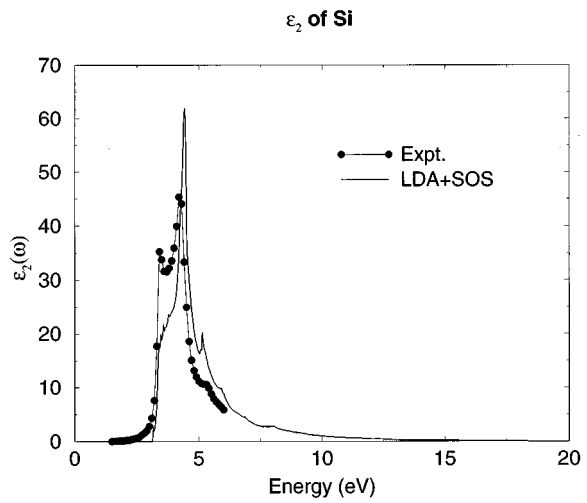

FIG. 3. Calculated imaginary part of the dielectric function of Si at the experimental equilibrium volume, shifted by $\Delta=0.6$ eV towards higher photon energies, compared with the experimental results of Ref. 3. The experimental E_1 structure at 4 eV is underestimated, whereas the main E_2 structure at 4.5 eV is overestimated.

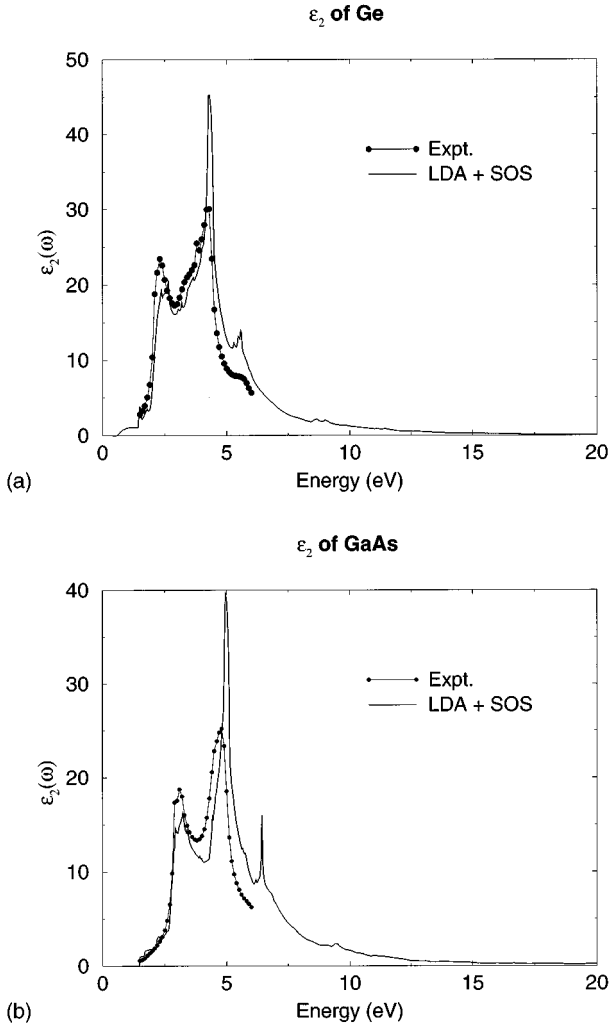

FIG. 4. Imaginary part of the dielectric function of Ge at 10 kbar shifts by 0.4 eV and GaAs at the experimental equilibrium volume shifted by 1.1 eV, compared with the experimental results of Ref. 3. In both Ge and GaAs $\epsilon_2(\omega)$, the experimental E_1 is only slightly underestimated and E_2 is overestimated.

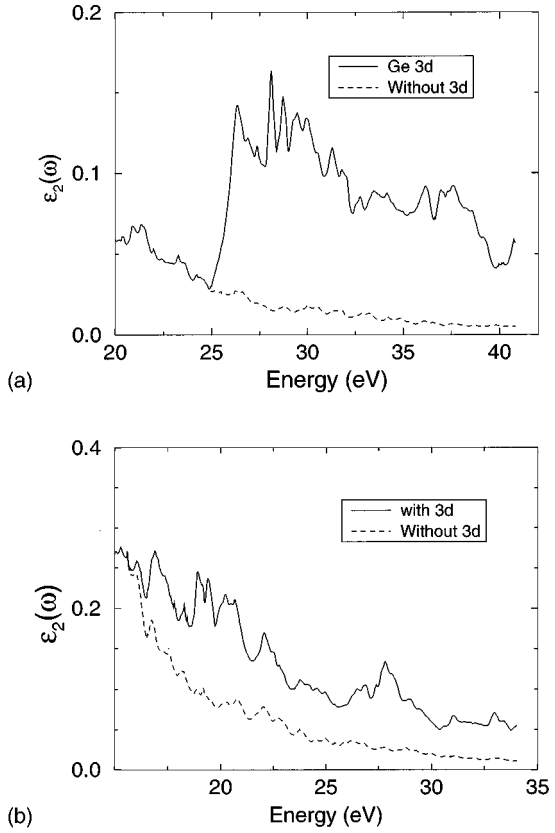

FIG. 5. Contribution of the $3d$ interband transitions to the imaginary part of the dynamical dielectric function of (a) Ge (at 10 kbar) and (b) GaAs at the experimental equilibrium volume. The full line and the dashed line are with and without $3d$ interband transitions, respectively. Due to narrow nature of the $3d$ semicore states of Ge, the intensity of ϵ_2 above 25 eV is very similar to the empty p-density of states of Ge, whereas for GaAs, the $3d$ semicore states of Ga are relatively delocalized, which makes the intensity of ϵ_2 above 12 eV much different from the Ga empty p density of states.

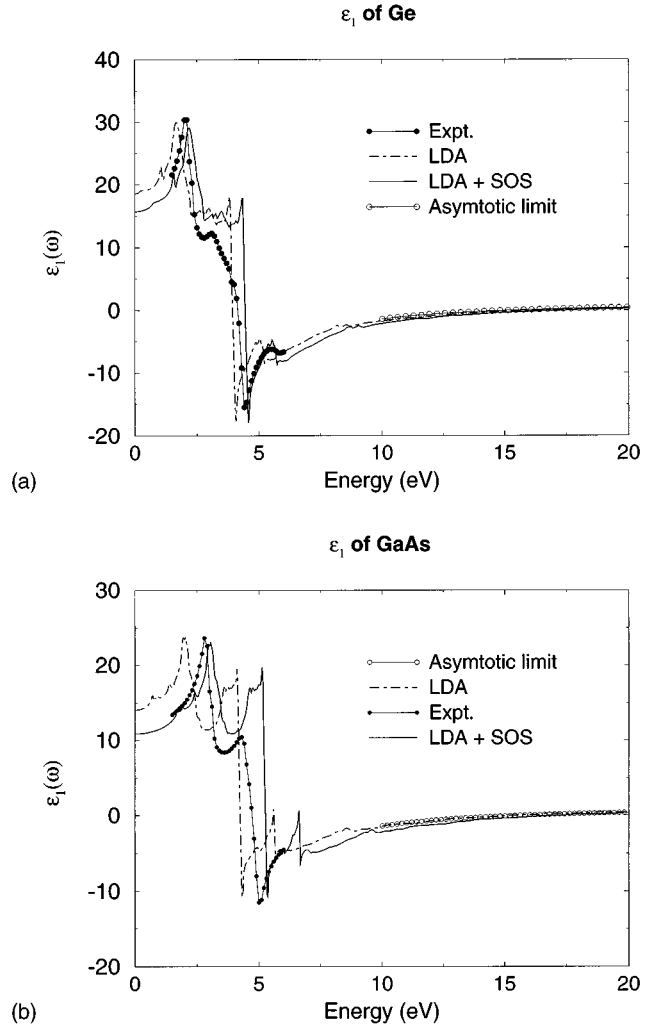

FIG. 6. Real part of the dielectric function of Ge (at 10 kbar) and GaAs, at the experimental equilibrium volume, compared with the experimental results of Ref. 3. The analytic asymptotic limit, shown by the empty circles, matches nicely the calculated spectra above 10 eV.

bitals used to describe the valence and conduction bands during the self-consistency. The large number of orbitals used is found necessary to obtain converged excited states up to 5 Ry above the top of the valence states. However, the total energy is insensitive to these high-energy orbitals, but the presence of the $3d$ core states of Ge and GaAs are important.[25]

Table II compares our band structure of Si for some high-symmetry points with some recent results from first-principles calculations based on pseudopotential and Gaussian orbitals methods.[27,28] We found good agreement between our results and these calculations. This reflects the high accuracy of our unoccupied states, which are used to determine the dynamical dielectric function.

Table III shows the calculated equilibrium structural parameters, i.e., the electronic pressure and the bulk modulus at the experimental unit cell volume V_0 and calculated cell volume V. The calculated equilibrium volume V is at the most 2% smaller than the experimental value, which corresponds to a less than 0.5% deviation from the experimental lattice parameter. However, the bulk modulus, which is very sensitive to the slope of the total energy versus the unit cell volume, deviates at the most by 10% in the case of Ge and when calculated at the experimental unit cell volume, but only by 5% when calculated at the theoretical equilibrium volume. Our calculation of the bulk modulus is in excellent agreement with other calculations.[34]

Figure 2 shows the LDA underestimated (a) direct band and (b) minimal gaps of Si, Ge, and GaAs compared with the Ge, and GaAs experimental results of Goñi, Syassen, and Cardona.[1] For GaAs a crossover from direct band gap to indirect band gap takes place between Γ and X at approximately 8 GPa. For Ge this crossover occurs along ΓL at a lower pressure of 3 GPa. The direct band gap increases linearly with pressure and is in good agreement with the experimental results for both GaAs and Ge. There is no experimental data for Si under hydrostatic pressure. Table IV present the first- and second-order coefficients describing the dependence of the direct band gap at Γ under hydrostatic pressure, $E_0(P)=E_0+aP+bP^2$ compared to the experimental results

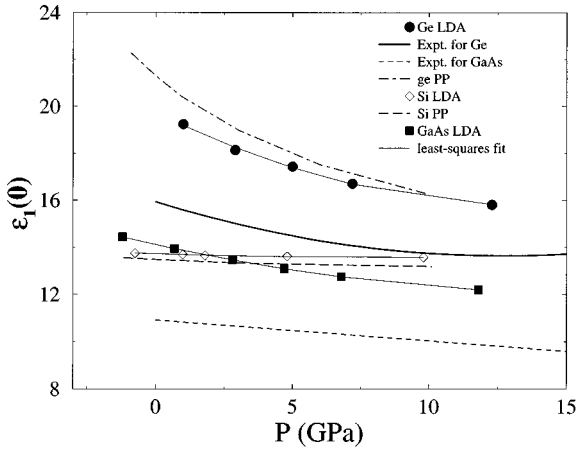

FIG. 7. LDA scalar-relativistic calculated static dielectric function of Si, Ge, and GaAs as a function of hydrostatic pressure compared to the experimental results of Goñi, Syassen, and Cardona (Ref. 1) and the pseudopotential calculation of Levine and Allan.[6]

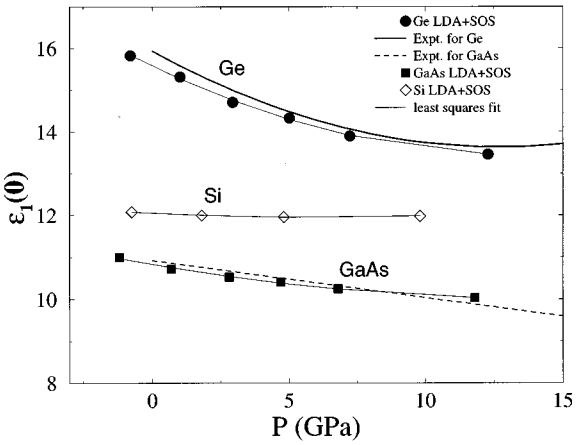

FIG. 8. LDA plus the scissors-operator shift (SOS) calculated static dielectric function of Si, Ge, and GaAs as a function of hydrostatic pressure compared to the experimental results of Goñi, Syassen, and Cardona (Ref. 1).

of Goñi, Syassen, and Cardona.[1] Apart from the underestimation of the band gap, the first and second coefficients of the pressure dependence of the band gap are in good agreement with the experimental results. This suggest that the scissors-operator shift is a good approximation for the description of the band gap under hydrostatic pressure.

IV. OPTICAL PROPERTIES OF Si, Ge, AND GaAs

A. Frequency dependence of the complex dielectric function of Si, Ge, and GaAs

Figure 3 and 4 present the imaginary part of the macroscopic dielectric function of Si, Ge, and GaAs obtained at the experimental ground-state lattice parameters except for Ge, where we have compressed the lattice parameter by about 1%. The compression is done because within the LDA and at the experimental lattice parameter Ge is a semimetal. The LDA ϵ_2 is shifted towards higher energy by the scissors-operator shift in order that the optical band gap agrees with experiment. The comparison to experimental results of Aspnes and Studna[3] shows that all the features in the experimental spectra are reproduced by the calculation. It is interesting to notice that the calculated LDA $\epsilon_2(\omega)$ of Si exhibits the largest underestimation of the E_1 peak (about 50% in intensity), whereas in Ge and GaAs the underestimation of the E_1 peak is only about 12%. The E_2 peak is overestimated by the LDA by about 34% for Si, 50% for Ge, and 60% for GaAs. This overestimation of the E_2 peak by the LDA is due to a strong van Hove singularity near the X points of the Brillouin zone where parallel bands occur over a large plateau.[5,35] This overestimation can be reduced substantially by including the lifetime broadening of the quasiparticles through a self-energy calculation.

The effect of interband electronic transitions due to the $3d$ semicore states, without scissors-operator shift, is presented in Fig. 5(a) and 5(b) for Ge and GaAs, respectively. For Ge the onset of transitions begins at a photon energy of about 25 eV and the intensity is very similar to the p density of states of the empty states of Ge. This is because the $3d$ states of Ge are very narrow and the dipole selection rules allow transitions only to the empty p states of Ge; the f states in this energy range are absent. For GaAs, the onset of transitions begins at 12 eV and the intensity ϵ_2 spectrum above 12 eV is very different from the empty p states of Ga. This is because of the relatively large dispersion of the $3d$ semicore states of Ga. It should be of interest to confirm experimentally these theoretical predictions.

The real part $\epsilon_1(\omega)$ of the dielectric function of Si, Ge, and GaAs calculated by the Kramers-Kronig transform of the imaginary part $\epsilon_2(\omega)$ is presented in Fig. 6 together with the experimental results of Aspnes and Studna.[3] In the same figure we have also presented the scissors-operator shift $\epsilon_1^{\mathrm{QP}}(\omega)$ and the high-frequency asymptotic limit

TABLE V. Calculated pressure, band gap, static dielectric function with and without scissors-operator shift (SOS), and the f-sum rule of Si as a function of volume (Ref. 28).

V_0/V	P (GPa)	f sum	Gap (eV)	ϵ_∞ (LDA)	ϵ_∞ (SOS)	ϵ_∞ (Expt.)
1.000	-0.75	0.988	0.50	13.75	12.08	12.0 [a]
1.025	1.8	0.989	0.46	13.65	12.00	
1.050	4.8	0.987	0.42	13.61	11.96	
1.100	9.8	0.991	0.34	12.57	11.98	

[a]Reference 38.

TABLE VI. Calculated pressure, band gap, static dielectric function with and SOS and the f-sum rule of Ge as a function of volume. The experimental data are from Goñi, Syassen, and Cardona (Ref. 1.)

V_0/V	P(GPa)	f sum	Gap (eV)	ϵ_∞ (LDA)	ϵ_∞ (SOS)	ϵ_∞ (Expt.)
1.025	1.0	1.053	0.04	19.24	15.32	15.59
1.050	2.9	1.041	0.21	18.14	14.71	15.01
1.075	5.0	1.042	0.29	17.44	14.33	14.49
1.100	7.2	1.043	0.37	16.70	13.90	14.07
1.150	12.3	1.045	0.48	15.81	13.46	13.63

TABLE VII. Calculated pressure, band gap, static dielectric function with and without SOS, and the f-sum rule of GaAs as a function of volume. The experimental data are from Goñi, Syassen, and Cardona (Ref. 1).

V_0/V	P (GPa)	f sum	Gap (eV)	ϵ_∞ (LDA)	ϵ_∞ (SOS)	ϵ_∞ (Expt.)
1.000	−1.2	1.041	0.29	14.44	11.0	11.05
1.025	0.68	1.042	0.48	13.93	10.72	10.88
1.050	2.8	1.043	0.66	13.45	10.53	10.69
1.075	4.7	1.044	0.85	13.09	10.41	10.53
1.100	6.8	1.044	1.02	12.75	10.25	10.34
1.150	11.8	1.046	1.08	12.20	10.03	9.90

TABLE VIII. First- and second-order coefficients describing the dependence of the static dielectric function on hydrostatic pressure [$\epsilon_\infty(P)=\epsilon_\infty^0+aP+bP^2$] for Si, Ge, and GaAs. The experimental data are from Goñi, Syassen, and Cardona (Ref. 1).

	ϵ_∞^0		a(1/GPa)		b (1/GPa^2)		$d\ln(\epsilon_\infty)/dP$ (10^{-12}/Pa)	
Semiconductor	Theor.	Expt.	Theor.	Expt.	Theor.	Expt.	Theor.	Expt.
Si	12.05		−0.032		0.0025		−2.65	
	11.16 [a]		−0.027[a]		0.0013[a]		−2.6, −2.43[a]	
Ge	15.58	15.94	−0.32	−0.36	0.012	0.014	−20.21	−22.60
	16.04[a]		−0.46[a]		0.018[a]		−31−28.66[a]	
GaAs	10.83	10.92	−0.11	−0.09	0.004		−10.43	−8.06

[a]Pseudopotential calculation of Ref. 6; slightly larger numbers are quoted for $d\ln(\epsilon_\infty)/dP$ in their Table VI.

TABLE IX. Calculated static dielectric function of Si, Ge, and GaAs at the equilibrium lattice parameter [except for Ge, where it is calculated at a slightly smaller lattice parameter (1% smaller) than the experimental one because Ge is a metal in LDA for $V/V_0 = 1$.]. The calculations are done using scalar relativistic (SR) LMTO without 3d states, with the 3d states (SR+3d), with the spin-orbit coupling at the variational level (SR+SO), and with the SO coupling and the 3d states included (SR+SO+3d).

	Si		Ge		GaAs	
	LDA	LDA+SOS	LDA	LDA+SOS	LDA	LDA+SOS
SR	13.75	12.08	18.14	14.71	14.44	11.0
SR+3d			18.16	14.73	14.47	11.03
SR+SO	13.69	12.0	18.52	14.23	14.90	10.52
SR+SO+3d			18.54	14.25	14.93	10.55
Expt.		12.0 [a] 11.4 [b]		14.98 [c]		10.9 [a]

[a]Reference 38.
[b]Reference 39.
[c]Reference 1.

$\epsilon_1(\omega)=1-\omega_P^2/\omega^2$, where ω_P is the free-electron plasmon frequency. We notice that the analytic asymptotic limit matches nicely the calculated LDA ϵ_1, which is an indication of the quality of the calculation. For the ϵ_1^{QP} we need to use a different plasmon frequency, as described in Eq. (14), due to the poor description of the higher excited states by the scissors approximation.

In conclusion, we believe that the excitonic effects may be important for the dielectric function of Si but less for those of Ge and GaAs. A QP calculation of the dielectric function including the dynamical screening of the Coulomb interaction, like in the *GW* approximation of Hedin,[16] would certainly improve the intensity of at least the E_2 peak by introducing a lifetime broadening of the quasiparticles.

B. Hydrostatic pressure dependence of the static dielectric function of Si, Ge, and GaAs

Figure 7 and 8 presents the hydrostatic pressure dependence of the static dielectric function ϵ_∞ of Si, Ge, and GaAs calculated within the LDA without and with the SOS, respectively. Our data are compared to the experimental results of Go$\tilde{\text{n}}$i, Syassen, and Cardona[1] and to the pseudopotential calculations of Si and Ge of Levine and Allan.[6] Our calculation and the pseudopotential theory of Ref. 6 suggest that the LDA overestimates the static dielectric function of Si, Ge, and GaAs over the whole range of hydrostatic pressure and that the use of a unique value of the scissors-operator shift for the correction of the band gap at Γ produces good agreement with the experimental results.[1] The static dielectric function decreases almost linearly with the pressure due to the increase of the direct band gap. However, for Si ϵ_∞ is almost constant with the pressure and this is because the increase of the direct band gap is almost compensated by a decrease of the indirect band gap (see Fig. 2).

Tables V, VI, and VII present the calculated pressure band gaps, static dielectric function, and *f*-sum rule for Si, Ge, and GaAs, with a comparison to the experimental results of Ref. 1. The agreement with the experimental results is excellent when the scissors-operator shift is used. The *f*-sum rule deviates at most by 5.2% from unity in the case of Ge, which reflects the high precision of the calculation of the optical matrix elements. The fact that the *f*-sum rule is not quite exhausted for Ge and GaAs (deviation of about 5%) as compared to Si (deviation of about 1%) is not due to a possible incompleteness of our basis set[36] but rather to our use of the all-electron electronic structure. When the valence states are very well isolated from the core states, like in the case of Si where the core states lie about 80 eV below the valence bands, the sum rule should be exhausted. However, for Ge and GaAs, where the semicore $3d$ states are very close to the valence states and greatly affect the optical properties, the *f*-sum rule could deviate markedly from unity, i.e., the average effective number of electrons per atom contributing to the optical transitions is much larger than four electrons per atom.[37] In pseudopotential theory, since the core states are absent, the *f*-sum rule is exhausted for all semiconductors.[6] The details of the contribution of the $3d$ semicore states to the oscillator strength and the study of the effective number of electrons contributing to the optical transitions are beyond the scope of this paper and will be addressed elsewhere.

The first- and second-order coefficients describing the pressure dependence of the static dielectric function ϵ_∞ are presented in Table VIII. The results are compared to the experimental results of Ref. 1 and the pseudopotential calculation of Ref. 6. The overall agreement with experiment and the pseudopotential calculation is excellent.

In Table IX we present our calculation for the static dielectric function of Si, Ge, and GaAs including the spin-orbit coupling effect at the variational level and the effect of the 3 *d* states in the interband transitions. The calculated potential includes always the $3d$ states and only the dielectric function is calculated with or without the $3d$ interband transitions. We have obtained that the inclusion of the $3d$ interband transitions increases slightly the static dielectric function, whereas the spin-orbit coupling increases it by 2.1% and 3.2% for Ge and GaAs, respectively. The ϵ_∞ of Si is insensitive to the spin-orbit coupling. The calculated scissors-operator shift ϵ_∞ including the spin-orbit coupling effect decreases by about 3.3% and 4.1% for Ge and GaAs, respectively. This is because the band gaps of Ge and GaAs are further reduced in the presence of spin-orbit coupling, which results in a larger scissors-operator shift for the determination of ϵ_∞^{QP}.

V. CONCLUSION

The macroscopic dielectric function in the random-phase-approximation without local-field effect has been implemented using the local-density approximation with an all-electron, full-potential linear muffin-tin orbital basis set. The method is used to calculate the optical properties of the semiconductors Si, Ge, and GaAs under hydrostatic pressure. We have found that the LDA overestimates the static dielectric function over the pressure range from 0 to 12 GPa and that a single value of the so-called scissors-operator shift, which accounts for the correct band gap at Γ, produces good agreement with the experimental data of Go$\tilde{\text{n}}$i, Syassen, and Cardona.[1] This leads us to conclude that because LDA underestimates the band gap, it is incapable of producing the correct static dielectric function even though ϵ_∞ is a ground-state property.

Since (i) the KS density functional (DF) without the local-density approximation should, in principle, produce the correct ϵ_∞ and (ii) the LDA calculation with the scissors-operator shift also produces the correct ϵ_∞, we are tempted to conclude that the KS-DF theory should produce the correct band gap for semiconductors. This conclusion is not confirmed by a non-self-consistent *GW* calculation, which suggests that the true KS-DF theory also underestimates the band gap.[18]

Our analysis of the dielectric function, the sum rules, and the energy-loss function shows that while the scissors-operator shift is a good approximation for the low-lying excited states, it appears as bad approximation for the high-energy excited states. This is because the high-energy states are free-electron-like, hence well described within the LDA.

Our calculation of the dynamical dielectric function shows that the E_1 peak intensity is underestimated for Si by about 50% and for Ge and GaAs by only 12%. These results

imply that the excitonic effects may be important for the dielectric function of Si, but less for those for Ge and GaAs.

We have also shown that including the $3d$ semicore states in the interband transitions hardly changes the static dielectric function ϵ_∞; however, their contribution to the intensity of the dynamical dielectric function for higher photon energies is substantial and could be checked experimentally. We have also found that the spin-orbit coupling has a significant effect on ϵ_∞ of Ge and GaAs, but not of Si.

ACKNOWLEDGMENTS

We thank J. W. Wilkins for interesting discussions. This research was supported in part by the U.S. Department of Energy Basic Energy Sciences, Division of Materials Sciences and by NSF, Grant No. DMR-9520319. Supercomputer time was provided by the Ohio State Supercomputer Center.

[1] A. R. Goñi, K. Syassen, and M. Cardona, Phys. Rev. B **41**, 10 104 (1990).
[2] L. Viña, S. Logothetidis, and M. Cardona, Phys. Rev. B **30**, 1979 (1984).
[3] D. E. Aspnes and A. A. Studna, Phys. Rev. B **27**, 985 (1983).
[4] S. Baroni and R. Resta, Phys. Rev. B **33**, 7017 (1986).
[5] M. Alouani, L. Brey, and N. E. Christensen, Phys. Rev. B **37**, 1167 (1988).
[6] Z. H . Levine and D. Allan, Phys. Rev. B **43**, 4187 (1991); Phys. Rev. Lett. **66**, 41 (1991).
[7] A. Dal Corso, S. Baroni, and R. Resta, Phys. Rev. B **49**, 5323 (1994).
[8] M. Chandrapal and F. H. Pollak, Solid State Commun. **18**, 1263 (1976); Phys. Rev. B **15**, 2127 (1977).
[9] W. R. Hanke and L. J. Sham, Phys. Rev. Lett. **33**, 582 (1974); Phys. Rev. B **21**, 4656 (1980).
[10] L. J. Sham, *Proceeding of the Fifteenth International Conference on the Physics of Semiconductors*, Kyoto, 1980 [J. Phys. Soc. Jpn. Suppl. A **49**, 69 (1980)].
[11] W. Hanke, H. J. Mattausch, and G. Strinati, in *Electron Correlations in Solids, Molecules, and Atoms*, edited by J. T. Devreese and F. Brosens (Plenum, New York, 1983).
[12] M. del Castello-Mussot and L. J. Sham, Phys. Rev. B **31**, 2092 (1985).
[13] S. G. Louie, J. R. Chelikowsky, and M. L. Cohen, Phys. Rev. Lett. **34**, 155 (1975).
[14] P. Hehenberg and W. Kohn, Phys. Rev. **136**, B864 (1964); W. Kohn and L. J. Sham, *ibid.* **140**, 1133 (1965).
[15] U. Von Barth and L Hedin, J. Phys. C **5**, 1629 (1972).
[16] L. Hedin, Phys. Rev. **139**, A796 (1965).
[17] M. S. Hybertsen and S. G. Louie, Phys. Rev. B **34**, 5390 (1986).
[18] R. W. Godby, M. Schlüter, and L. J. Sham, Phys. Rev. B **37**, 10 159 (1988).
[19] J. P. Perdew and M. Levy, Phys. Rev. Lett. **51**, 1884 (1983); R. W. Godby, M. Schlüter, and L. J. Sham, *ibid.* **56**, 2415 (1986).
[20] C. S. Wang and B. M. Klein, Phys. Rev. B **24**, 3417 (1981).
[21] M. Huang and W. Y. Ching, Phys. Rev. B **47**, 9449 (1993).
[22] O. K. Andersen, Phys. Rev. B **12**, 3060 (1975).
[23] J. M. Wills (unpublished).
[24] Here the principal quantum number ν and the spin channel σ are ignored for simplicity; however, our numerical code has the spin polarization capability, and the use of the different ν with the same momentum channel in the basis set. We also use only one κ variational parameter per orbital (see definition in the text) in all formulas to avoid using it as an obvious index to the wave function and extra summation in the Bloch wave function.
[25] G. B. Bachelet and N. E. Christensen, Phys. Rev. B **31**, 879 (1985).
[26] N. E. Christensen, Phys. Rev. B **30**, 5753 (1984).
[27] C. T. Chan, D. Vanderbilt, and S. G. Louie, Phys. Rev. B **33**, 2455 (1986) and references therein.
[28] M. Rohlfing, P. Krüger, and J. Pollmann, Phys. Rev. B **48**, 17 791 (1993).
[29] S. L. Adler, Phys. Rev. **126**, 413 (1962); N. Wiser, *ibid.* **129**, 62 (1963).
[30] H. Ehrenreich and M. L. Cohen, Phys. Rev. **115**, 786 (1959).
[31] O. Jepsen and O. K. Andersen, Solid State Commun. **9**, 1763 (1971); G. Lehmann and M. Taut, Phys. Status Solidi **54**, 469 (1972).
[32] A. B. Chen, Phys. Rev. B **14**, 2384 (1976).
[33] R. Del Sole and R. Girlanda, Phys. Rev. B **48**, 11 789 (1993).
[34] M. Methfessel, Phys. Rev. B **38**, 1537 (1988).
[35] J. R. Chelikowsky and M. L. Cohen, Phys. Rev. Lett. **31**, 1582 (1973).
[36] We have checked carefully the basis set by increasing the number of Hankel functions for negative kinetic energies and Neumann functions for positive kinetic energies κ^2 and have not been able to improve on the f-sum rule. Our basis set indicates that all physical properties quantities have converged, including the total energy, which converged at the tenth mRy level.
[37] For more information see H. R. Philipp and H. Ehrenreich, Phys. Rev. **129**, 1550 (1963).
[38] W. A. Harrison, *Electronic Structure and the Properties of Solids* (Freeman, San Fransisco, 1980).
[39] H. H. Li, J. Chem. Phys. Data **9**, 561 (1980).
[40] G. E. Engel and B. Farid, Phys. Rev. B **46**, 15 812 (1992).